

# NEUTRINO EMISSION DUE TO ELECTRON BREMSSTRAHLUNG IN SUPERFLUID NEUTRON-STAR CORES

A.D. KAMINKER

A.F. Ioffe Physical Technical Institute, 194021 St.Petersburg, Russia  
E-mail: kam@astro.ioffe.rssi.ru

AND

P. HAENSEL

N. Copernicus Astronomical Center, Bartycka 18, 00-716 Warszawa, Poland  
E-mail: haensel@camk.edu.pl

published in: *Acta Physica Polonica B* **30** (1999) 1125

We study neutrino energy emission rates (emissivities) due to electron bremsstrahlung produced by  $ee$  and  $ep$  collisions in the superfluid neutron star cores. The neutrino emission due to  $ee$  collisions is shown to be the dominant neutrino reaction at not too high temperatures ( $T \lesssim 10^8$  K) in dense matter if all other neutrino reactions involving nucleons are strongly suppressed by neutron and proton superfluidity. Simple practical expressions for the  $ee$  and  $ep$  neutrino emissivities are obtained. The efficiency of various neutrino reactions in the superfluid neutron-star cores is discussed for the cases of standard neutrino energy losses and the losses enhanced by the direct Urca process.

PACS numbers: 97.60.Jd, 26.60.+c, 23.40.Bw

## 1. Introduction

In the first  $10^5$  years of their life, neutron stars (NSs) cool mainly via neutrino emission from their cores. This emission results from weak interaction processes involving baryons and leptons. It is important, thus, to study various neutrino reactions. For simplicity, we will mainly consider the NS cores composed of neutrons  $n$ , with some admixture of protons  $p$  and electrons  $e$ . The neutrino reactions in the neutron-star cores are tradi-

tionally divided into two groups, which differ drastically by their efficiency and produce the *standard* or *rapid* cooling (e.g., ref. [1]).

The standard cooling is mainly provided by the neutron and proton branches of the modified Urca reactions [2, 3]

$$n + N \rightarrow p + N + e + \bar{\nu}_e, \quad p + e + N \rightarrow n + N + \nu_e, \quad (1)$$

where  $N$  is a nucleon ( $n$  or  $p$ ), and by the nucleon–nucleon ( $nn$ ,  $np$ , and  $pp$ ) bremsstrahlung processes

$$N + N \rightarrow N + N + \nu + \bar{\nu}. \quad (2)$$

The rapid cooling is strongly enhanced by the direct Urca processes

$$n \rightarrow p + e + \bar{\nu}_e, \quad p + e \rightarrow n + \nu_e, \quad (3)$$

which can operate [4] only in the central regions of rather massive NSs with proton fraction exceeding 11% of the total baryon density. If the direct Urca reaction is allowed (in a non-superfluid NS), the neutrino emissivity is typically 4–5 orders of magnitude higher than in the standard reactions (1) and (2).

It is widely accepted (see, e.g., [5, 6] and references therein), that neutrons and protons in a NS core can be in a superfluid state. The superfluidity is generally thought to be of BCS type, produced by attractive component of nuclear forces. Various microscopic theories predict very different critical temperatures of neutron and proton superfluids,  $T_{cn}$  and  $T_{cp}$ , which range from  $10^8$  to  $10^{10}$  K. The neutron superfluidity in the NS cores is generally believed to be produced by triplet-state pairing of neutrons (with anisotropic superfluid energy gap), while the proton superfluidity is due to the singlet-state pairing (with isotropic gap). If  $T \ll T_{cn}$  and  $T \ll T_{cp}$  the superfluidity strongly suppresses all the neutrino reactions (1)–(3) involving nucleons (e.g., [1, 3, 7]).

Onset of the neutron or proton superfluidity with the decrease of temperature in a cooling NS initiates also an additional specific neutrino reaction which can be considered as neutrino production due to Cooper pairing of quasinucleons  $\tilde{N}$

$$\tilde{N} + \tilde{N} \rightarrow \nu + \bar{\nu}. \quad (4)$$

The emission due to singlet-state pairing of neutrons has been calculated by Flowers et al. [8] and Voskresensky & Senatorov [9, 10] while the emission due to triplet-state pairing of neutrons and singlet-state pairing of protons has been determined by Yakovlev et al. [11, 12] and Kaminker et al. [13]. The effect is much stronger for neutrons than for protons due to the smallness of axial–vector electroweak currents for protons.

In contrast to the non-superfluid cores, where the main neutrino emission is produced either by the modified or by the direct Urca processes (depending on the equation of state and density), very different neutrino mechanisms can dominate in the superfluid cores, depending on the relative magnitudes of  $T$ ,  $T_{cn}$  and  $T_{cp}$ . In particular, Cooper-pair neutrino emission (4) can be very important if  $0.1 T_{cN} \lesssim T \lesssim T_{cN}$  (e.g., ref. [12]). At lower temperatures,  $T \ll T_{cN}$ , this emission falls exponentially.

On the other hand, as mentioned by Schaab et al. [14], an additional neutrino emission mechanism, the neutrino-pair bremsstrahlung due to  $ep$  scattering

$$e + p \rightarrow e + p + \nu + \bar{\nu} , \quad (5)$$

can be important in the superfluid NS cores. This mechanism, and the closely related mechanism of neutrino bremsstrahlung due to  $ee$  scattering

$$e + e \rightarrow e + e + \nu + \bar{\nu} \quad (6)$$

has been considered briefly by Kaminker et al. [15]. The latter authors have estimated the neutrino energy emission rates (emissivities) in these reactions using simplified criteria of similarity of neutrino emission and electron conduction processes. It is quite evident that these reactions, especially the neutrino  $ee$  bremsstrahlung, can be important in highly superfluid NS cores, where all the reactions involving nucleons are drastically suppressed by the nucleon superfluidity. Thus, rigorous calculation of the emissivities in the reactions (5) and (6) deserves special study.

Notice that the neutrino bremsstrahlung due to  $ee$  scattering of nondegenerate electrons at not too high densities,  $\rho \lesssim 10^{10} \text{ g cm}^{-3}$  (corresponding to the outer NS crust), was considered by Cazzola & Saggion [16, 17]. The authors obtained general but cumbersome expressions for the emissivity [16] and performed numerical calculations using Monte Carlo method [17]. The main result of their consideration was that the emissivity due to the  $ee$  bremsstrahlung did not exceed 1% of the total emissivity from other neutrino reactions in a NS crust (pair annihilation, photoneutrino and plasmon decay). We will show that this is not so in a NS core.

The aim of the present article is to carry out an accurate calculation of the neutrino emissivities for the bremsstrahlung reactions (5) and (6), and to analyze the efficiency of various neutrino production mechanisms (1)–(6) in superfluid NS cores.

## 2. Superfluid neutron-star cores

Mass density of the matter in a NS core is expected to range from about  $0.5\rho_0$  at its outer edge [18], to  $(5\text{--}10)\rho_0$  at the stellar center, where  $\rho_0 = 2.8 \times 10^{14} \text{ g cm}^{-3}$  is the saturation density of nuclear matter. At  $\rho \lesssim 2\rho_0$ , neutron-star matter consists mostly of neutrons, with a few percent admixture of protons, electrons, and possibly muons. The fraction of muons is usually much smaller than that of electrons, and a simple *npe* model is a good approximation. At higher densities,  $\rho \gtrsim 2\rho_0$ , other particles may appear, such as hyperons, condensed pions or kaons, or even free (deconfined) quarks. Neutrino emissivity of dense neutron-star matter with different compositions has been reviewed by Pethick [1]. For simplicity, we will neglect possible presence of hyperons and exotic particles, and consider *npe* matter only. All constituents of the matter are strongly degenerate. The electrons form an ultrarelativistic and almost ideal gas, with the electron Fermi-momentum

$$p_{Fe} = \hbar(3\pi^2 n_e)^{1/3} = 648.6 (n_e/n_0)^{1/3} m_e c, \quad (7)$$

where  $n_e$  and  $m_e$  are electron number density and mass, respectively, and  $n_0 = 0.16 \text{ fm}^{-3}$  is the standard nuclear saturation density. The electron Fermi energy (chemical potential) is  $\mu_e \approx p_{Fe}c \approx (100\text{--}300) \text{ MeV}$ . Neutrons and protons are nonrelativistic and form strongly interacting Fermi liquids. The condition of beta-equilibrium implies that the chemical potentials of particles satisfy the equality  $\mu_n = \mu_p + \mu_e$ . Charge neutrality leads to the equality of proton and electron number densities ( $n_p = n_e$ ) and Fermi momenta ( $p_{Fe} = p_{Fp}$ ). The Fermi energy of neutrons is close to that of electrons, while the Fermi energy of protons is much smaller (typically, 3–30 MeV).

Both nucleon species,  $n$  and  $p$ , can be in a superfluid state (Sect. 1). Microscopically, the superfluidity leads to the appearance of the energy gap  $\Delta$  in the nucleon dispersion relation. For a triplet-state neutron superfluid, the gap is anisotropic along the neutron Fermi surface. For a singlet-state pairing of protons the gap is isotropic. The proton gap  $\Delta_p = \Delta_p(T)$  depends only on temperature  $T$ . In the frame of the BCS theory (which we adopt further on), the proton critical temperature  $T_{cp}$  is related to the zero-temperature energy gap  $\Delta_p(0)$  by  $T_{cp} = \Delta_p(0)/(1.764 k_B)$  [19], where  $k_B$  is the Boltzmann constant.

Superfluidity of neutrons and protons suppresses the main neutrino generation mechanisms (1)–(3) in the NS core and opens an additional neutrino reaction (4). Strong superfluidity of neutrons and protons ( $T_{cn} \gg T$  and  $T_{cp} \gg T$ ) suppresses drastically all neutrino reactions (1)–(5) involving nucleons. Superfluidity of protons affects even the neutrino *ee* bremsstrahlung (6), (not very strongly), by changing screening of *ee* interaction.

The plasma screening momentum  $q_s$  in  $npe$  matter is given by (e.g., ref. [20])

$$y_s^2 \equiv \frac{q_s^2}{4p_{Fe}^2} = \frac{e^2}{\pi \hbar c} \left( 1 + \frac{m_p^* p_{Fp}}{m_e^* p_{Fe}} D_p \right) \quad (8)$$

where  $m_e^* = \mu_e/c^2$  and  $m_p^*$  is an effective proton mass (which determines the proton density of states near the Fermi level and which can differ from the bare mass  $m_p$  due to polarization effects in dense matter). The first term in brackets comes from the electron screening, while the second term is due to the proton screening. The latter term contains the function  $D_p$ . For nonsuperfluid protons ( $T \geq T_{cp}$ ) one has  $D_p = 1$ , while for  $T < T_{cp}$  the factor  $D_p$  describes superfluid reduction of proton screening. Gnedin & Yakovlev [20] fitted numerical values of this factor, calculated for singlet-state proton pairing, by

$$D_p = \left( 0.9443 + \sqrt{(0.0557)^2 + (0.1886y)^2} \right)^{1/2} \times \exp \left( 1.753 - \sqrt{(1.753)^2 + y^2} \right), \quad (9)$$

where  $y = \Delta_p(T)/(k_B T)$ . According to Levenfish & Yakovlev [21] the parameter  $y$  at any  $T < T_{cp}$  is given by the fitting expression

$$y = \sqrt{1 - \frac{T}{T_{cp}}} \left( 1.456 - 0.157 \sqrt{\frac{T_{cp}}{T}} + 1.764 \frac{T_{cp}}{T} \right). \quad (10)$$

### 3. General formalism of neutrino $ep$ and $ee$ bremsstrahlung

Consider two neutrino bremsstrahlung mechanisms (5) and (6) for strongly degenerate, relativistic electrons and strongly degenerate, nonrelativistic protons. We will treat these processes using the standard perturbation theory of weak interactions. We will use the units in which  $c = \hbar = k_B = 1$  and return to ordinary physical units in the final expressions.

The emissivities  $Q_{ep}$  and  $Q_{ee}$  [erg cm<sup>-3</sup> s<sup>-1</sup>] of the processes (5) and (6) can be written as

$$Q_{12} = \frac{\zeta_{12}}{(2\pi)^{14}} \int d\mathbf{p}_1 \int d\mathbf{p}_2 \int d\mathbf{p}'_1 \int d\mathbf{p}'_2 \int d\mathbf{k}_\nu \int d\mathbf{k}'_\nu \times \delta^{(4)}(P_1 + P_2 - P'_1 - P'_2 - K) \omega f_1 f_2 (1 - f'_1)(1 - f'_2) W, \quad (11)$$

where  $P_1 = (\varepsilon_1, \mathbf{p}_1)$  and  $P_2 = (\varepsilon_2, \mathbf{p}_2)$  are 4-momenta of two charged particles before scattering,  $P'_1 = (\varepsilon'_1, \mathbf{p}'_1)$  and  $P'_2 = (\varepsilon'_2, \mathbf{p}'_2)$  are 4-momenta of the

same particles after scattering. Index 1 labels an electron and index 2 labels either a proton or a second electron;  $\zeta_{ep} = 1$ ,  $\zeta_{ee} = 1/2$  (to avoid double counting of the same  $ee$  scattering events). The quantities  $K_\nu = (\omega_\nu, \mathbf{k}_\nu)$  and  $K'_\nu = (\omega'_\nu, \mathbf{k}'_\nu)$  are 4-momenta of neutrino and antineutrino, respectively, and  $K = K_\nu + K'_\nu = (\omega, \mathbf{k})$  is 4-momentum of the neutrino pair ( $\omega = \omega_\nu + \omega'_\nu$  and  $\mathbf{k} = \mathbf{k}_\nu + \mathbf{k}'_\nu$ ). Furthermore,

$$f_i = \left[ 1 + \exp \left( \frac{\varepsilon_i - \mu_i}{T} \right) \right]^{-1} \quad (12)$$

is a Fermi-Dirac distribution of a particle before scattering ( $i=1, 2$ ), and  $f'_i$  is the corresponding distribution for a particle after scattering. The  $\delta$ -function describes 4-momentum conservation. Finally,  $W$  is the differential transition rate

$$W = \frac{G_F^2}{2} \frac{\sum_{\sigma, \nu} |M_{12}|^2}{(2\omega_\nu)(2\omega'_\nu)(2\varepsilon_1)(2\varepsilon_2)(2\varepsilon'_1)(2\varepsilon'_2)} , \quad (13)$$

where  $G_F = 1.436 \times 10^{-49}$  erg cm<sup>3</sup> is the Fermi weak interaction constant, and  $|M_{12}|^2$  is the squared transition amplitude. Summation is over spin states of charged particles before and after scattering  $\sigma = (\sigma_1, \sigma_2, \sigma'_1, \sigma'_2)$  and over the neutrino flavors  $\nu = (\nu_e, \nu_\mu, \nu_\tau)$ . The neutrino energies are assumed to be much lower than the intermediate boson mass ( $\sim 80$  GeV). The processes in question are represented by four ( $ep$  scattering) or eight ( $ee$  scattering) Feynman diagrams. Each diagram includes a neutrino-pair emission four-tail vertex. The amplitudes are

$$M_{ep} = M_A, \quad M_{ee} = M_A - M_B , \quad (14)$$

where

$$M_A = 4\pi e^2 l^\alpha \left[ \frac{1}{t_{22} - q_s^2} (\bar{u}'_2 \gamma^\beta u_2) (\bar{u}'_1 L_{\alpha\beta}^{(1)} u_1) + \frac{1}{t_{11} - q_s^2} (\bar{u}'_1 \gamma^\beta u_1) (\bar{u}'_2 L_{\alpha\beta}^{(2)} u_2) \right] , \quad (15)$$

$$M_B = 4\pi e^2 l^\alpha \left[ \frac{1}{t_{21} - q_s^2} (\bar{u}'_1 \gamma^\beta u_2) (\bar{u}'_2 L_{\alpha\beta}^{(3)} u_1) + \frac{1}{t_{12} - q_s^2} (\bar{u}'_2 \gamma^\beta u_1) (\bar{u}'_1 L_{\alpha\beta}^{(4)} u_2) \right] , \quad (16)$$

$$L_{\alpha\beta}^{(1)} = \Gamma_{e\alpha} G_e(P'_1 + K) \gamma_\beta + \gamma_\beta G_e(P_1 - K) \Gamma_{e\alpha} ,$$

$$L_{\alpha\beta}^{(2)} = \Gamma_{2\alpha} G_2(P'_2 + K) \gamma_\beta + \gamma_\beta G_2(P_2 - K) \Gamma_{2\alpha} ,$$

$$\begin{aligned}
L_{\alpha\beta}^{(3)} &= \Gamma_{e\alpha} G_e(P'_2 + K) \gamma_\beta + \gamma_\beta G_e(P_1 - K) \Gamma_{e\alpha} , \\
L_{\alpha\beta}^{(4)} &= \Gamma_{e\alpha} G_e(P'_1 + K) \gamma_\beta + \gamma_\beta G_e(P_2 - K) \Gamma_{e\alpha} , 
\end{aligned} \tag{17}$$

$$\Gamma_e^\alpha = C_{eV} \gamma^\alpha + C_{eA} \gamma^\alpha \gamma^5 , \quad \Gamma_p^\alpha = C_{pV} \gamma^\alpha + C_{pA} \gamma^\alpha \gamma^5 , \tag{18}$$

$l^\alpha = (\bar{\psi}_\nu \gamma^\alpha (1 + \gamma^5) \psi_\nu)$  is neutrino 4-current;  $u_1, u'_1, u_2$  and  $u'_2$  denote standard bispinor amplitudes of charged particles;  $\psi_\nu$  and  $\bar{\psi}_\nu$  are the standard bispinor amplitudes of emitted neutrinos; upper bar denotes a Dirac conjugate, Greek indices  $\alpha$  and  $\beta$  run over (0,1,2,3),  $\gamma^\alpha$  and  $\gamma^5$  are Dirac matrices;  $G_e(P)$  and  $G_p(P)$  are the electron and proton propagators  $G_i(P) = (P_\alpha \gamma^\alpha + m_i)/(P^2 - m_i^2)$ . We use the bare proton mass  $m_2 = m_p$  in the proton propagator and in the normalization of the proton bispinor amplitudes  $\bar{u}_p u_p = 2m_p$  in Eqs. (15) and (17). It will be shown that the final results are independent of  $m_p$  which is a consequence of nonrelativistic approximation for protons. Nevertheless the results do depend on the proton density of states near the Fermi level, i.e., on  $m_p^*$ . An additional term  $M_B$  in  $M_{ee}$  appears due to identity of colliding electrons; it contains four diagrams with interchanged final electron states. In Eqs. (15) and (16) we have used photon propagators in the Feynman gauge [22] and four familiar kinematic invariants

$$\begin{aligned}
t_{11} &= (P_1 - P'_1)^2, & t_{22} &= (P_2 - P'_2)^2, \\
t_{21} &= (P_2 - P'_1)^2, & t_{12} &= (P_1 - P'_2)^2,
\end{aligned} \tag{19}$$

where  $t_{11}$  and  $t_{12}$  are the standard kinematic invariants denoted usually as  $t$  and  $u$ . We have added the squared screening momentum  $q_s^2$  (see Sect. 2) to the kinematic invariants in the denominators of Eqs. (15) and (16) to account for the plasma screening effects. Furthermore, in Eq. (18)  $C_{iV}$  and  $C_{iA}$  are, respectively, the vector and the axial vector weak coupling constants associated with four-tail neutrino-emission vertices on electron ( $i = e$ ) or proton ( $i = p$ ) lines of the Feynman diagrams. For emission of  $\nu_e \bar{\nu}_e$  pairs at  $i = e$  (charged + neutral currents), one has  $C_{eV} = 2 \sin^2 \theta_W + 0.5$  and  $C_{eA} = 0.5$ , while for emission of  $\nu_\mu \bar{\nu}_\mu$  and  $\nu_\tau \bar{\nu}_\tau$  (neutral currents only),  $C'_{eV} = 2 \sin^2 \theta_W - 0.5$  and  $C'_{eA} = -0.5$ . In this case,  $\theta_W$  is the Weinberg angle,  $\sin^2 \theta_W \simeq 0.23$ . Neutrino emission for  $i = p$  goes only via neutral currents and we have  $C_{pV} = (1 - 4 \sin^2 \theta_W)/2 \approx 0.04$  and  $C_{pA} = 1.26/2 = 0.63$ , independently of neutrino flavors.

In our case, neutrino-pair momentum is sufficiently small ( $k \sim T \ll p_{Fe}$ ), so that we can use the approximation of Festa & Ruderman [23] for the electron propagators:

$$G_e(P' + K) = \frac{P'_\alpha \gamma^\alpha}{2(P'K)} , \quad G_e(P - K) = -\frac{P_\alpha \gamma^\alpha}{2(PK)} \tag{20}$$

and the nonrelativistic approximation for the proton propagators

$$G_p(P'_2 + K) = -G_p(P_2 - K) = \frac{1 + \gamma^0}{2\omega} . \quad (21)$$

The standard tedious calculations using the Lenard identity [22]

$$\begin{aligned} & \int d\mathbf{k}_\nu \int d\mathbf{k}'_\nu \delta^{(4)}(K - K_\nu - K'_\nu) \frac{K_\nu^\alpha K'^\beta_\nu}{\omega_\nu \omega'_\nu} \\ &= \frac{\pi}{6} (K^2 g^{\alpha\beta} + 2K^\alpha K^\beta) , \end{aligned} \quad (22)$$

yield

$$\begin{aligned} Q_{12} &= \frac{e^4 G_F^2}{12(2\pi)^{11}} \zeta_{12} \int d\mathbf{p}_1 \int d\mathbf{p}_2 \int d\mathbf{p}'_1 \int d\mathbf{p}'_2 \frac{\omega}{\varepsilon_1 \varepsilon'_1 \varepsilon_2 \varepsilon'_2} \\ &\times J_{12} f_1 f_2 (1 - f'_1)(1 - f'_2) . \end{aligned} \quad (23)$$

For  $ep$  scattering we have

$$J_{ep} = \frac{2^6 C_{e+}^2 m_p^2}{(t_{22} - q_s^2)^2} \frac{K^2 (P_1 P'_1) (2\varepsilon_1 \varepsilon'_1 - P_1 P'_1)}{(P_1 K)(P'_1 K)} , \quad (24)$$

where  $C_{e+}^2 = \sum_\nu (C_{eV}^2 + C_{eA}^2)$ . Notice that  $Q_{ep}$  determined by Eqs. (23) and (24) appears to be very similar to the emissivity  $Q_{br}$  given by Eqs. (A7) and (A13) in the article by Haensel et al. [24] who considered neutrino bremsstrahlung due to Coulomb scattering of electrons by atomic nuclei in the NS crust. Equation (24) describes only neutrino emission associated with electron lines of the Feynman diagrams and does not include analogous emission associated with proton lines (the second term in Eq. (15)) which vanishes in the limit of nonrelativistic protons.

In the case of  $ee$  scattering we have

$$J_{ee} = C_{e+}^2 K^2 (J_1 + J_2 - J_3) , \quad (25)$$

where

$$\begin{aligned} J_1 &= X_1 - I_1 , \quad J_2 = X_2 - I_2 , \quad J_3 = Y_1 + Y_2 + Z_1 + Z_2 , \\ I_1 &= \frac{2^6}{(t_{11} - q_s^2)(t_{22} - q_s^2)} \left[ (P_1 P_2)(P'_1 P'_2) + \frac{C_{e-}^2}{C_{e+}^2} (P_1 P'_2)(P_2 P'_1) \right] \\ &\times \left[ \frac{(P'_1 P'_2)}{(P'_1 K)(P'_2 K)} + \frac{(P_1 P_2)}{(P_1 K)(P_2 K)} - \frac{(P_1 P'_2)}{(P_1 K)(P'_2 K)} - \frac{(P_2 P'_1)}{(P_2 K)(P'_1 K)} \right] , \\ X_1 &= 2^6 [(P_1 P_2)(P'_1 P'_2) + (P_2 P'_1)(P_1 P'_2)] \end{aligned}$$



$$\begin{aligned}
& \times \left[ \frac{1}{(t_{22} - q_s^2)^2} \frac{(P_1 P'_1)}{(P_1 K)(P'_1 K)} + \frac{1}{(t_{11} - q_s^2)^2} \frac{(P_2 P'_2)}{(P_2 K)(P'_2 K)} \right], \\
Y_1 &= \frac{2^6 (P_1 P_2)(P'_1 P'_2)}{(t_{11} - q_s^2)(t_{12} - q_s^2)} \\
& \times \left[ \frac{(P'_1 P'_2)}{(P'_1 K)(P'_2 K)} - \frac{(P_2 P'_1)}{(P_2 K)(P'_1 K)} - \frac{(P_2 P'_2)}{(P_2 K)(P'_2 K)} \right], \\
Z_1 &= \frac{2^6 (P_1 P_2)(P'_1 P'_2)}{(t_{22} - q_s^2)(t_{12} - q_s^2)} \\
& \times \left[ \frac{(P_1 P_2)}{(P_1 K)(P_2 K)} - \frac{(P_1 P'_1)}{(P_1 K)(P'_1 K)} - \frac{(P_2 P'_1)}{(P_2 K)(P'_1 K)} \right], \tag{26}
\end{aligned}$$

where  $C_{e-}^2 = \sum_\nu (C_{eV}^2 - C_{eA}^2)$ . The expressions for  $I_2$  and  $X_2$  are obtained from those for  $I_1$  and  $X_1$  by replacing  $1 \rightleftharpoons 2$ . The expressions for  $Y_2$  and  $Z_2$  are obtained from those for  $Y_1$  and  $Z_1$  by replacing  $1 \rightleftharpoons 2$  and  $1' \rightleftharpoons 2'$  simultaneously. The quantities defined in Eqs. (26) possess numerous symmetry properties. For instance,  $X_1$  is invariant with respect to replacing  $1 \rightleftharpoons 2$  and  $1' \rightleftharpoons 2'$ , etc. The integrand in (23) can be shown to be highly symmetric as well. Using the symmetry properties one can easily prove that in Eq. (23) it is sufficient to use the expression

$$J_{ee} = 2 C_{e+}^2 K^2 (X - I_1 - Y_1 - Z_1). \tag{27}$$

In this case

$$X = 2^7 \frac{(P_1 P_2)(P'_1 P'_2) + (P_2 P'_1)(P_1 P'_2)}{(t_{22} - q_s^2)^2} \frac{(P_1 P'_1)}{(P_1 K)(P'_1 K)} \tag{28}$$

corresponds to “direct”  $ee$  scattering, i.e., to square of any single term (amplitude) in  $M_A$  or  $M_B$  in Eqs. (14)–(16);  $I_1$  corresponds to interference of amplitudes with exchanging electrons 1 and 2 ( $1 \rightleftharpoons 2, 1' \rightleftharpoons 2'$ ); while  $Y_1$  and  $Z_1$  correspond to interference of amplitudes with mutually transposed electron final states  $1' \rightleftharpoons 2'$ .

For further analysis, it is convenient to introduce an appropriate 4-momentum transfer  $Q = P'_2 - P_2 = P_1 - P'_1 - K = (\Omega, \mathbf{q})$  from particle 1 to particle 2 due to Coulomb interaction. Using the 4-momentum conserving delta-function in Eq. (11) we can remove the integration over  $\mathbf{p}'_1$  and over  $\omega$ , and then replace the integration over  $\mathbf{p}'_2$  by the integration over  $\mathbf{q}$ . It is convenient also to express  $Q_{ep}$  and  $Q_{ee}$  in the form suggested by Haensel et al. [24] for the emissivity  $Q_{br}$  of the neutrino bremsstrahlung due to scattering of electrons off atomic nuclei in the NS envelopes:

$$Q_{12} = \frac{8\pi G_F^2 e^4 C_{e+}^2}{567} T^6 n_2 L_{12}. \tag{29}$$

In a Coulomb liquid of atomic nuclei, a dimensionless quantity  $L_{12}$  has meaning of a Coulomb logarithm. For neutrino  $ee$  and  $ep$  bremsstrahlung, we are interested in,  $L_{12}$  is a dimensionless function to be evaluated. General expressions for  $L_{12}$  are

$$L_{ep} = \frac{567}{(2\pi)^{10} T^6 p_{\text{Fe}}^3} \int d\mathbf{p}_1 \int d\mathbf{p}_2 \int d\mathbf{q} \int d\mathbf{k} \frac{\omega}{\varepsilon_1 \varepsilon'_1} \\ \times \frac{K^2}{(q^2 + q_s^2)^2} \frac{(P_1 P'_1)(2\varepsilon_1 \varepsilon'_1 - P_1 P'_1)}{(P_1 K)(P'_1 K)} f_1 f_2 (1 - f'_1)(1 - f'_2) , \quad (30)$$

$$L_{ee} = \frac{567}{2^{16} \pi^{10} T^6 p_{\text{Fe}}^3} \int d\mathbf{p}_1 \int d\mathbf{p}_2 \int d\mathbf{q} \int d\mathbf{k} \frac{\omega}{\varepsilon_1 \varepsilon'_1 \varepsilon_2 \varepsilon'_2} \\ \times K^2 (X - I_1 - Y_1 - Z_1) f_1 f_2 (1 - f'_1)(1 - f'_2) . \quad (31)$$

To obtain Eq. (30) we set  $\varepsilon_2 \varepsilon'_2 = m_p^2$  in the denominator of (23) because the protons are nonrelativistic.

Since charged particles are strongly degenerate, the main contribution to  $L_{12}$  comes from those transitions, in which the particle momenta before and after collisions lie in the narrow thermal shells around their Fermi surfaces,  $|\varepsilon - \mu| \lesssim T$ . In Eqs. (30) and (31) we may set  $d\mathbf{p}_i = m_i^* p_{\text{Fi}} d\varepsilon_i d\Omega_i$ , where  $d\Omega_i$  is solid angle element in the direction of  $\mathbf{p}_i$ . We also put  $\varepsilon_1 = p_1$  in Eqs. (30) and (31), and  $\varepsilon_2 = p_2$  in Eq. (31), respectively, since electrons are ultrarelativistic.

Following Haensel et al. [24] we introduce the quantities  $\mathbf{q} = \mathbf{q}_t + \mathbf{q}_r$ ,  $\mathbf{k} = \mathbf{k}_t + \mathbf{k}_r$  and  $\mathbf{p}'_1 = \mathbf{p}_1 - \mathbf{q}_t = \mathbf{p}'_1 + \mathbf{q}_r + \mathbf{k}$ , where  $\mathbf{q}_t$  corresponds to purely elastic Coulomb scattering while  $\mathbf{q}_r$  takes into account inelasticity; vector  $\mathbf{p}'_1$  is directed along  $\mathbf{q}_r$  but has the same length as  $\mathbf{p}_1$ , i.e.,  $|\mathbf{p}'_1| = |\mathbf{p}_1|$ ;  $\mathbf{k}_r$  and  $\mathbf{k}_t$  are the orthogonal vector components parallel and perpendicular to  $\mathbf{p}'_1$ , respectively. Notice that  $q_t = 2p_1 \sin(\vartheta/2)$ , where  $\vartheta$  is an angle between  $\mathbf{p}_1$  and  $\mathbf{p}'_1$ . Strong electron degeneracy implies  $q_r \ll p_{\text{Fe}}$ ,  $k \ll p_{\text{Fe}}$  and  $\Omega \ll p_{\text{Fe}}$ , although  $q_t$  can be comparable to  $p_{\text{Fe}}$  for large-angle electron scattering events. From geometrical consideration and energy-momentum conservation in analogy with expressions given by Haensel et al. [24] we obtain

$$q^2 = (\mathbf{q}_t + \mathbf{q}_r)^2 = q_t^2 + q_r^2 - q_t^2 (q_r/p_{\text{Fe}}) , \\ P_1 P'_1 \approx (q_t^2 + k_t^2 + 2\mathbf{q}_t \cdot \mathbf{k})/2 , \\ P_1 K \approx p_1(q_r - \Omega) - \mathbf{q}_t \cdot \mathbf{k}, \quad P'_1 K \approx p_1(q_r - \Omega) , \\ \Omega + \omega = \varepsilon_1 - \varepsilon'_1 \approx q_r + k_r , \\ K^2 = \omega^2 - k_r^2 - k_t^2 \approx k_0^2 - k_t^2 . \quad (32)$$

Here,  $k_0^2 = (q_r - \Omega)(2\omega - q_r + \Omega)$ , and the condition  $K^2 > 0$  yields  $k_0 \geq k_t$  and  $q_r \geq \Omega$ ,  $\omega \geq (q_r - \Omega)/2 \geq 0$ .

In what follows, we consider  $ep$  and  $ee$  scattering separately.

#### 4. Neutrino $ep$ bremsstrahlung

Let us evaluate  $Q_{ep}$  from Eqs. (29) and (30):

$$L_{ep} = \frac{567m_p^*}{(2\pi)^{10}T^6} \int d\varepsilon_1 \int d\varepsilon_2 \int d\Omega_1 \int d\Omega_2 \int_0^{2\pi} d\varphi_q \int_0^{2p_{Fe}} dq_t q_t \int_{-\infty}^{\infty} dq_r \int_{(q_r-\Omega)/2}^{\infty} d\omega \int_0^{2\pi} d\varphi \int_0^{k_0} dk_t k_t f_1 f_2 (1-f'_1) (1-f'_2) \times \frac{\omega}{\varepsilon_1 \varepsilon'_1} \frac{(k_0^2 - k_t^2)}{(q_t^2 + q_r^2 - \Omega^2 + q_s^2)^2} \frac{q_t^2 [1 - q_t^2/(4p_{Fe}^2)]}{(q_r - \Omega)(q_r - \Omega - \mathbf{q}_t \cdot \mathbf{k}/p_{Fe})}, \quad (33)$$

where we have introduced integration over  $d\mathbf{q} = d\varphi_q dq_t q_t dq_r$  with cylindrical axis along  $\mathbf{p}_1$  and integration over  $d\mathbf{k} = d\varphi dk_t dk_t d\omega$  with cylindrical axis along  $\mathbf{p}_1''$ . In the latter integration we have used the equality  $dk_r = d\omega$ ;  $\varphi$  is an azimuthal angle of  $\mathbf{k}$  with respect to the  $\mathbf{p}_1''$ -axis.

Consider the case of  $q_s \ll p_{Fe}$  typical for the NS cores, where  $q_s$  is the plasma screening momentum (Sect. 2). Integration in Eq. (33) can be simplified because the main contribution comes from the values  $q_s \lesssim q \ll p_{Fe}$  which correspond to the *small-angle approximation*. In this approximation, we can omit  $q_t^2/(2p_{Fe})^2$  in the numerator and  $\mathbf{q}_t \cdot \mathbf{k}/p_{Fe}$  in the denominator of the integrand. Furthermore we may set  $1/(\varepsilon_1 \varepsilon'_1) = 1/p_{Fe}^2$  in the integrand of (33) and take into account that the energy transfer  $\Omega$  from an electron to a proton is

$$\Omega = \varepsilon_2 - \varepsilon'_2 \approx \frac{1}{m_p^*} \left( \mathbf{p}_2 \cdot \mathbf{q} + \frac{q^2}{2} \right) \approx \frac{p_{Fe} q}{m_p^*} \cos \vartheta_{q2}, \quad (34)$$

where  $\vartheta_{q2}$  is an angle between  $\mathbf{q}$  and  $\mathbf{p}_2$ . Then the integrand in Eq. (33) depends only on the relative positions of  $\mathbf{p}_2$  and  $\mathbf{q}$ .

First we can fix positions of  $\mathbf{p}_1$ ,  $\mathbf{p}_2$  and  $\mathbf{q}$  and perform the following integrations:

$$\int_0^{2\pi} d\varphi \int_0^{k_0} dk_t k_t (k_0^2 - k_t^2) = 2\pi(q_r - \Omega)^2 \left[ \omega - \frac{1}{2}(q_r - \Omega) \right]^2. \quad (35)$$

A sequence of angular integrations yields  $\int d\Omega_1 \int d\varphi_q \int d\Omega_2 \dots = 16\pi^3 \int d\cos \vartheta_{q2} \dots$ . Finally, we are left with the only angular integration in Eq. (33), that over  $d\cos \vartheta_{q2}$ . According to Eq. (34), the variation range of  $\cos \vartheta_{q2}$  is

related to variation range of  $\Omega$ . Let us consider two extreme cases.

*Low temperature limit* ( $T \ll q_s p_{Fe}/m_p^* \ll q_s$ ) corresponds to thermal energies  $T$  much less than recoil energy of protons. This case is most important for practical use [15]. Let us replace integration over  $\cos \vartheta_{q2}$  by integration over  $\Omega$ :  $\cos \vartheta_{q2} = m_p^* \Omega / (q_t p_{Fe})$ , where  $(q_r - 2\omega) \leq \Omega \leq q_r$ . The Pauli principle strongly restricts possible values of  $\Omega$  as well as final states of electrons and protons.

The condition  $T \ll q_s$  leads to the inequalities  $q_r \ll q_t$ ,  $\omega \ll q_t$ ,  $\Omega \ll q_t$ . The integration over  $dq_t$  in Eq. (33) yields

$$\int_0^{2p_{Fe}} dq_t \frac{q_t^2}{(q_t^2 + q_s^2)^2} \simeq \frac{1}{2p_{Fe}} \left( \frac{\pi}{4y_s} - 1 \right), \quad (36)$$

where  $y_s$  is given by Eq. (8).

The integrations over  $\varepsilon_1$  and  $\varepsilon_2$  are standard:

$$\begin{aligned} & \int_{-\infty}^{+\infty} d\varepsilon_1 \int_{-\infty}^{+\infty} d\varepsilon_2 f_1 f_2 (1 - f'_1) (1 - f'_2) \\ &= \frac{(\omega + \Omega)}{e^{(\omega + \Omega)/T} - 1} \frac{\Omega}{1 - e^{-\Omega/T}} \quad \text{for } \Omega > 0, (\omega + \Omega) > 0; \\ &= \frac{(|\Omega| - \omega)}{1 - e^{-(|\Omega| - \omega)/T}} \frac{|\Omega|}{e^{|\Omega|/T} - 1} \quad \text{for } \Omega < 0, (\omega + \Omega) < 0, \end{aligned} \quad (37)$$

where  $\varepsilon'_1 = \varepsilon_1 - \omega - \Omega$  and  $\varepsilon'_2 = \varepsilon_2 + \Omega$ . Now we are left with integrations over  $d\omega d\Omega dq_r$  in six domains restricted by the inequalities  $q_r \geq \Omega$  and  $\omega \geq (q_r - \Omega)/2 \geq 0$  (see Eqs. (32)). Three of them correspond to  $q_r > 0$  [(a)  $\Omega \geq 0$ ; (b)  $\Omega < 0$ ,  $\omega + \Omega \geq 0$ ; (c)  $\omega + \Omega < 0$ ], while three others correspond to  $0 \geq q_r \geq \Omega$  [(d)  $\omega + \Omega \geq 0$ ; (e)  $2\omega + \Omega \geq 0 > \omega + \Omega$ ; (f)  $0 > 2\omega + \Omega \geq q_r$ ]. Following Haensel et al. [24] we can introduce dimensionless variables  $u = q_r/T$ ,  $w = \Omega/T$ ,  $v = \omega/T$ ,  $v_0 = (q_r - \Omega)/(2T)$ . Six domains of integration over  $dv dw dv_0$  in Eq. (33) are reduced to four ones, and integration over  $dv_0$  is trivial ( $\int_0^v dv_0 (v - v_0)^2 = v^3/3$ ).

Finally, using Eqs. (33), (35), (36), and (37) we obtain

$$L_{ep} \approx \frac{189 m_p^{*2} T^2}{2^7 \pi^5 p_{Fe}^4 y_s} \eta = \frac{3\pi^3}{40 y_s} \left( \frac{m_p^* T}{p_{Fe}^2} \right)^2 \xi, \quad (38)$$

where

$$\eta = \int_0^\infty dv v^4 \left\{ \int_0^\infty dw \frac{w(v+w)}{(e^{v+w} - 1)(1 - e^{-w})} \right.$$

$$\begin{aligned}
& + \int_0^v dw \frac{w(v+w)}{(e^{v+w}-1)(1-e^{-w})} + \int_0^v dw \frac{w(v-w)}{(e^{v-w}-1)(e^w-1)} \\
& + \int_{2v}^\infty dw \frac{w(v-w)}{(1-e^{v-w})(e^w-1)} \Big\} \approx 1646.7, \quad (39)
\end{aligned}$$

as obtained by numerical integration, and  $\xi = 315 \eta / (16\pi^8) \approx 3.417$ .

Kaminker et al. [15] proposed to estimate  $L_{ep}$  by rescaling the Coulomb logarithm  $L_{br}$  calculated by Haensel et al. [24] for scattering of ultrarelativistic degenerate electrons by atomic nuclei in liquid state. In the context of  $ep$  scattering,  $L_{br}$  is valid at  $T_{Fp} \ll T \ll T_{Fe}$ . The rescaling procedure has been based on the similarity criterion:  $L_{ep} = L_{br} \nu_{ep} / \nu_{ep}^{(0)}$ , where  $\nu_{ep}$  is an effective  $ep$  collision frequency for the conditions under consideration ( $T \ll q_s \lesssim T_{Fp} \ll T_{Fe}$ ) and  $\nu_{ep}^{(0)}$  is an effective frequency of elastic  $ep$  collisions at  $T \gg q_s$  (e.g., [25]). For  $T \ll q_s$ , the authors used the collision frequency  $\nu_{ep}$  that determines the electron thermal conductivity (e.g., [20]). One can easily verify that the result given by Eqs. (38) and (39) differs from the crude estimate by Kaminker et al. [15] by a small factor  $y_s^2$  given by (8). Thus Kaminker et al. [15] have strongly (typically, by two orders of magnitude) overestimated  $Q_{ep}$ , obtained in the present paper by an accurate evaluation. The nature of this overestimation comes from using the effective thermal-conduction collision frequency  $\nu_{ep}$  in the rescaling procedure. The thermal conduction at  $T \ll q_s$  is associated with small momentum transfers ( $q \sim T$ ). Corresponding collision frequency appears to be greatly enhanced as compared to the frequency of collisions with higher momentum transfers ( $q \sim q_s$ ) which should have been used in rescaling. For instance, it would be appropriate to use the  $ep$  collision frequency which determines electron electric conductivity (e.g., [26]). Therefore, the rescaling proposed in ref. [15] is basically correct if one uses physically justified effective collision frequencies.

Finally, we obtain (in the standard physical units)

$$\begin{aligned}
Q_{ep} &= \frac{\pi^4 \xi G_F^2 e^4 C_{e+}^2 m_p^{*2}}{945 \hbar^9 c^8 y_s p_{Fe}^4} n_p (k_B T)^8 R_{ep} \\
&\approx \frac{3.69 \times 10^{14}}{y_s} \left( \frac{m_p^*}{m_p} \right)^2 \left( \frac{n_0}{n_p} \right)^{1/3} R_{ep} T_9^8 \text{ erg cm}^{-3} \text{ s}^{-1}. \quad (40)
\end{aligned}$$

Here we have introduced the factor  $R_{ep}$  that describes suppression of the emissivity by the proton superfluidity. We introduced also  $T_9 \equiv T/10^9$  K.

If protons are normal ( $T \geq T_{cp}$ ), one has  $R_{ep} = 1$  in Eq. (40). The factor  $R_{ep}$  reduces neutrino emission at  $T < T_{cp}$ . It should be the same as the factor  $R_{np}$  that describes reduction of the bremsstrahlung neutrino

emission in  $np$  collisions by proton superfluidity [3]:

$$\begin{aligned}
R_{ep} &= \frac{1}{2.732} \left[ A \exp \left( 1.306 - \sqrt{(1.306)^2 + y^2} \right) \right. \\
&\quad \left. + 1.732 B^7 \exp \left( 3.303 - \sqrt{(3.303)^2 + 4y^2} \right) \right], \\
A &= 0.9982 + \sqrt{(0.0018)^2 + (0.3815y)^2}, \\
B &= 0.3949 + \sqrt{(0.6051)^2 + (0.2666y)^2}, \tag{41}
\end{aligned}$$

where  $y = \Delta/T$  (Sect. 2).

*Moderate temperature limit* ( $q_s p_{Fe}/m_p^* \ll T \ll q_s$ ). In this case thermal energy is much higher than the recoil energy of protons. Therefore, as follows from Eq. (34),  $T \gg \Omega$ . To estimate  $L_{ep}$  in this limit we can omit  $\Omega$  in comparison with all quantities  $\sim T$  in the integrand and in the integration limits in Eq. (33). Note that the condition  $k_0^2 \approx q_r(2\omega - q_r) \geq 0$  obviously gives  $q_r \geq 0$  and  $\omega \geq q_r/2$ . Then we easily perform integrations in Eq. (35) and subsequent integrations over  $d\Omega_2 d\varphi_q$  and  $d\Omega_1$ . In the limit of  $\Omega \rightarrow 0$  standard integration yields

$$\int d\varepsilon_1 \int d\varepsilon_2 f_1 f_2 (1 - f'_1) (1 - f'_2) = \frac{\omega T}{e^{\omega/T} - 1}. \tag{42}$$

which gives

$$\begin{aligned}
L_{ep} &= \frac{567 m_p^* T}{24 \pi^6 p_{Fe}^2} \int_0^{2p_{Fe}} dq_t \frac{q_t^3}{(q_t^2 + q_s^2)^2} \int_0^\infty du \int_{u/2}^\infty dv \frac{v^2 (v - u/2)^2}{e^v - 1} \\
&= 3 \left( \frac{m_p^* T}{p_{Fe}^2} \right) L_{ep}^{(0)}, \\
L_{ep}^{(0)} &= \int_0^{2p_{Fe}} dq_t \frac{q_t^3}{(q_t^2 + q_s^2)^2} \approx \ln \left( \frac{1}{y_s} \right) - \frac{1}{2}. \tag{43}
\end{aligned}$$

Here  $L_{ep}^{(0)}$  is close to the Coulomb logarithm for neutrino bremsstrahlung due to collisions of electrons with nondegenerate protons in the low-temperature limit ( $T_{Fe} \lesssim T \ll q_s \ll T_{Fe}$ ). The factor  $3m_p^* T/p_{Fe}^2$  in Eq. (43) appears due to degeneracy of protons in the case considered here. As a result, we obtain the emissivity (in the standard physical units)

$$\begin{aligned}
Q_{ep} &= \frac{8\pi G_F^2 e^4 C_{e+}^2 m_p^*}{189 \hbar^9 c^8 p_{Fe}^2} n_p (k_B T)^7 L_{ep}^{(0)} R_{ep} \\
&\approx 1.89 \times 10^{17} \left( \frac{m_p^*}{m_p} \right) \left( \frac{n_p}{n_0} \right)^{1/3} L_{ep}^{(0)} R_{ep} T_9^7 \text{ erg cm}^{-3} \text{ s}^{-1}. \tag{44}
\end{aligned}$$

Note that at *low temperatures*  $Q_{ep}$  has the temperature dependence  $Q_{ep} \propto T^8$ , which differs from the case of *moderate temperatures*,  $Q_{ep} \propto T^7$ , as well as from the case of nondegenerate protons,  $Q_{ep} \propto T^6$  ( $T \gtrsim T_{Fp}$ ).

The case  $q_s \ll T \lesssim T_{Fp}$  has no importance for astrophysical applications. It can be shown that in this case the emissivity is again given by Eq. (44) with somewhat different (temperature dependent) Coulomb logarithm  $L_{ep}^{(0)}$ .

### 5. Neutrino $ee$ bremsstrahlung

Let us consider now the neutrino emissivity  $Q_{ee}$  for  $ee$  bremsstrahlung. We restrict ourselves by the same condition  $q_s \ll p_{Fe}$  (small-angle approximation) as for  $ep$  bremsstrahlung. In contrast to the previous case, only the region of relatively small temperatures,  $T \ll q_s$ , is important for practical applications.

The integrand in Eq. (31) depends on the relative positions of  $\mathbf{p}_1$ ,  $\mathbf{p}_2$ ,  $\mathbf{q}$  and  $\mathbf{k}$ . In particular it depends on angle  $\Theta$  between  $\mathbf{p}_1$  and  $\mathbf{p}_2$ . Thus we may direct  $\mathbf{p}_1$  along the  $z$ -axis and place  $\mathbf{p}_2$  in the  $(xz)$ -plane. Let  $(\vartheta_{q1}, \varphi_q)$  be polar angles of  $\mathbf{q}$  and  $(\vartheta_{k1}, \varphi_k)$  be polar angles of  $\mathbf{k}$ . Let us introduce also an angle  $\vartheta_{q2}$  between  $\mathbf{q}$  and  $\mathbf{p}_2$ , an angle  $\vartheta_{k2}$  between  $\mathbf{k}$  and  $\mathbf{p}_2$ , and a relative azimuthal angle  $\varphi_{kq}$  between  $\mathbf{k}$  and  $\mathbf{q}$ .

We can use relations (32) as for  $ep$  bremsstrahlung. While evaluating the right hand side of Eq. (31) it is useful to introduce also an additional auxiliary integral  $\int d\Omega \delta(\varepsilon_2 - \varepsilon'_2 + \Omega)$ . Using the relation  $\varepsilon'_2 = |\mathbf{p}_2 + \mathbf{q}| \approx p_2(1 + (q/p_{Fe}) \cos \vartheta_{q2})$  we can present the  $\delta$ -function under this integral in the form

$$\delta(\varepsilon_2 - \varepsilon'_2 + \Omega) \approx \frac{1}{q} \delta\left(\cos \vartheta_{q2} - \frac{\Omega}{q}\right). \quad (45)$$

Equations (31), (26), (28), (32), and (45) yield

$$\begin{aligned} L_{ee} = L_{ee}^{(1)} - L_{ee}^{(2)} &\approx \frac{567}{2^9 \pi^{10} T^6 p_{Fe}} \int d\varepsilon_1 \int d\varepsilon_2 \int d\Omega_1 \int d\Omega_2 \int_0^{2\pi} d\varphi_q \\ &\times \int_0^{2p_{Fe}} dq_t q_t \int_0^\infty dq_r \int_{-\infty}^{q_r} d\Omega \int_0^{2\pi} d\varphi \int_{(q_r - \Omega)/2}^\infty d\omega \int_0^{k_0} dk_t k_t \\ &\times \frac{1}{q} \delta\left(\cos \vartheta_{q2} - \frac{\Omega}{q}\right) \frac{(1 - \cos \Theta)^2}{(q_t^2 + q_r^2 - \Omega^2 + q_s^2)^2} \frac{(k_0^2 - k_t^2) q_t^2}{(q_r - \Omega)^2} \\ &\times \left[ 1 - \frac{1 + (C_{e-}/C_{e+})^2}{2} \frac{(q_r - \Omega)}{\omega - k \cos \vartheta_{k2}} \right] \omega f_1 f_2 (1 - f'_1)(1 - f'_2). \quad (46) \end{aligned}$$

Here we have introduced the same notations as in Eq. (33), and we have divided  $L_{ee}$  into two parts,  $L_{ee}^{(1)}$  and  $L_{ee}^{(2)}$ . The first part,  $L_{ee}^{(1)}$ , corresponds to the first term (equal to 1) in square brackets which comes from  $X$  in Eq. (31) (“direct”  $ee$  scattering). The second part,  $L_{ee}^{(2)}$ , corresponds to the second term which comes from  $I_1$  in Eq. (31) (interference of amplitudes with exchanging electrons 1 and 2). It can be shown that the terms  $Y_1$  and  $Z_1$  in Eq. (31) (interference of amplitudes with mutually transposed electron final states) contain small parameters  $\sim q_r/p_{Fe}$  and  $\sim (q_t/p_{Fe})^2$  and can be neglected.

Let us use the relationship  $\cos \vartheta_{q2} = \cos \Theta \cos \vartheta_{q1} + \sin \Theta \sin \vartheta_{q1} \cos \varphi_q$  in Eq. (45) and express  $\cos \vartheta_{q2}$  in the  $\delta$ -function through integration variables  $q_t, q_r, \varphi_q$ , and  $\Theta$  in Eq. (46). We also need to express  $\cos \vartheta_{k2}$  through  $k_r, k_t, \varphi$ , and  $\Theta$ . For this purpose we take into account additional approximate relations (justified at  $p_{Fe} \gg q_t$ )

$$\begin{aligned}\cos \vartheta_{q2} &\approx (q_r \cos \Theta + q_t \sin \Theta \cos \varphi_q)/q, \\ \cos \vartheta_{k2} &\approx (k_r \cos \Theta + k_t \sin \Theta \cos \varphi_k)/k, \\ \cos \varphi_k &\approx \sin \varphi_{kq} \approx \sin \varphi.\end{aligned}\tag{47}$$

The third relationship is valid at  $q_r \ll q_s \lesssim q_t$ ,  $\Omega \ll q_t$ , and  $\omega \ll q_t$ . First we evaluate  $L_{ee}^{(1)}$  in Eq. (46). The integration over  $d\varphi$  is trivial, the integration over  $k_t$  is reduced to (35), and the integration over  $d\varphi_q$  can be done with help of the delta-function

$$\delta\left(\cos \vartheta_{q2} - \frac{\Omega}{q}\right) = \frac{q}{q_t \sin \Theta} \delta\left(\cos \varphi_q - \frac{\Omega - q_r \cos \Theta}{q_t \sin \Theta}\right).\tag{48}$$

Now we can integrate over  $d\Omega_1$  and  $d\Omega_2$  in a straightforward manner:

$$\int_{4\pi} \int_{4\pi} d\Omega_1 d\Omega_2 (1 - \cos \Theta)^2 (\sin \Theta)^{-1} = 12\pi^3.\tag{49}$$

The integrations over  $d\varepsilon_1$  and  $d\varepsilon_2$  can be performed using Eq. (37). We are left with a 4-dimensional integral (over  $d\omega d\Omega dq_r dq_t$ ). Using Eq. (36) and introducing the same dimensionless variables as in Eqs. (38) and (39), we obtain

$$L_{ee}^{(1)} \approx \frac{567 T^2}{28\pi^5 p_{Fe}^2 y_s} \eta = \frac{3\pi^3}{16 y_s} \left(\frac{T}{p_{Fe}}\right)^2 \xi_1,\tag{50}$$

where  $\eta$  is defined by Eq. (39) and  $\xi_1 = 189\eta/(16\pi^8) = 2.05$ .

Making use of Eqs. (47) and performing straightforward but tedious calculations we can also evaluate  $L_{ee}^{(2)}$ . It appears to contain a small numerical



factor  $\approx 0.05$  as compared to  $L_{ee}^{(1)}$ . Note that we have neglected other interference terms in Eq. (31) which could be of the same order of magnitude or even larger than  $L_{ee}^{(2)}$ . Therefore we will use only the main term (50) for applications.

Finally the neutrino emissivity  $Q_{ee}$  can be written in the form (in the standard units)

$$\begin{aligned} Q_{ee} &= \frac{\pi^4 \xi_1 G_F^2 e^4 C_{e+}^2}{378 \hbar^9 c^{10} y_s p_{Fe}^2} n_e (k_B T)^8 \\ &\approx \frac{0.69 \times 10^{14}}{y_s} \left( \frac{n_e}{n_0} \right)^{1/3} T_9^8 \text{ erg cm}^{-3} \text{ s}^{-1}. \end{aligned} \quad (51)$$

As in the case of  $Q_{ep}$ , this result differs from a crude estimate given by Kaminker et al. [15] by a small factor  $y_s^2 \ll 1$  due to an unfortunate use of inappropriate thermal-conduction  $ee$  collision frequency in the rescaling procedure.

Let us emphasize that the emissivity  $Q_{ep}$  is reduced exponentially by strong proton superfluidity, while  $Q_{ee}$  is affected by the superfluidity in a much weaker manner, only through the plasma screening parameter (8). If protons are normal, they provide the major contribution into the plasma screening. If they are strongly superfluid, a weaker electron screening becomes important, which *enhances*  $Q_{ee}$ , but not to a great extent (see below).

Let us remind that the neutrino emissivity  $Q_{ee}$  for nondegenerate electrons in the neutron star crusts has been calculated by Cazzola & Sagion [16, 17]. We have compared their numerical results (Fig. 2 in ref. [17]) with our Eq. (51) for several temperatures ( $T_9 = 5, 7, 8, 10$ ) at those values of  $\rho \gtrsim 10^8 \text{ g cm}^{-3}$ , where the relativistic electrons start to become degenerate and both approaches are expected to be qualitatively valid. We have obtained reasonable agreement of the results.

Finally let us make a few remarks about neutrino bremsstrahlung reactions involving muons,  $\mu^-$ . Muons can appear in sufficiently dense matter of neutron star cores, provided the electron number density exceeds the threshold value  $n_e > (m_\mu c)^3 / (3\pi^2 \hbar^3) = 0.0052 \text{ fm}^{-3}$ , where  $m_\mu$  is the muon mass. For realistic equations of state, this happens at  $\rho \gtrsim (1.5\text{--}2) \rho_0$ . The muons, like electrons, form almost ideal degenerate gas, but they are mainly non-relativistic (near the threshold density) or mildly relativistic at much higher densities. Beta-equilibrium condition implies  $\mu_\mu = \mu_e$ , where  $\mu_\mu$  is the muon chemical potential. The number density of muons is much smaller than the number density of neutrons or electrons for all densities. In muonic matter, several new neutrino bremsstrahlung reactions are allowed, resulting from  $\mu e$ ,  $\mu\mu$ ,  $\mu p$  scattering. The neutrino emissivities in these reactions

can be evaluated in the same manner as the emissivities due to  $ep$  and  $ee$  neutrino bremsstrahlung.

For instance, in the nonrelativistic limit ( $p_{F\mu} \ll m_\mu c$ ) at  $T \ll q_s$ , in analogy with Eq. (40), we obtain

$$\begin{aligned} Q_{e\mu} &= \frac{\pi^4 \xi G_F^2 e^4 C_{e+}^2 m_\mu^2}{945 \hbar^9 c^8 y_s p_{F\mu}^3 p_{Fe}} n_\mu (k_B T)^8 \\ &\approx \frac{4.68 \times 10^{12}}{y_s} \left( \frac{n_0}{n_e} \right)^{1/3} T_9^8 \text{ erg cm}^{-3} \text{ s}^{-1}, \end{aligned} \quad (52)$$

where  $n_\mu$  is the muon number density. Equation (52) differs from Eq. (40) by a small factor  $(m_\mu/m_p^*)^2$ .

One can see that, under considered conditions, the neutrino emissivity  $Q_{e\mu}$  is much smaller than the emissivity  $Q_{ee}$  due to  $ee$  scattering (cf. Eqs. (52) and (51)).

Our estimates show that the neutrino bremsstrahlung reactions involving muons are less efficient than analogous reactions involving electrons, for all densities typical for neutron star cores.

## 6. Discussion

Let us discuss the efficiency of various neutrino emission mechanisms in superfluid NS cores. For illustration, we adopt a moderately stiff equation of state proposed by Prakash et al. [27] (the version with compression modulus  $K_0 = 180$  MeV and with the same simplified symmetry energy  $S_V$  which was used by Page & Applegate [28]). We assume that dense neutron-star matter consists of neutrons, protons and electrons (no muons and hyperons). The nucleon effective masses will be set equal to 0.7 of the masses of bare particles. The equation of state allows the direct Urca process to operate at  $\rho \geq 4.64 \rho_0$ . We consider two densities,  $\rho = 2 \rho_0$ , as an example of the standard neutrino cooling (the direct Urca is forbidden), and  $\rho = 5 \rho_0$ , representing the case of the cooling enhanced by the direct Urca process. Both nucleon species, neutrons and protons, are supposed to form superfluids. We consider a triplet-state neutron pairing ( $^3P_2$ ), with zero projection of the total momentum ( $m_J = 0$ ) of a Cooper pair onto quantization axis, and a singlet-state proton pairing ( $^1S_0$ ). Since the critical temperatures  $T_{cn}$  and  $T_{cp}$  of both superfluids, as calculated from microscopic theories, are very model dependent (e.g., refs. [5, 6, 29-32]), we do not make any specific choice of microscopic superfluid model but treat  $T_{cn}$  and  $T_{cp}$  as free parameters.

Figures 1 and 2 show temperature dependence of the neutrino emissivities for various neutrino production mechanisms at  $\rho = 2\rho_0$  and  $\rho = 5\rho_0$ , respectively, assuming rather strong neutron and moderate proton superfluids,  $T_{cn} = 8 \times 10^9$  K and  $T_{cp} = 2.5 \times 10^9$  K.

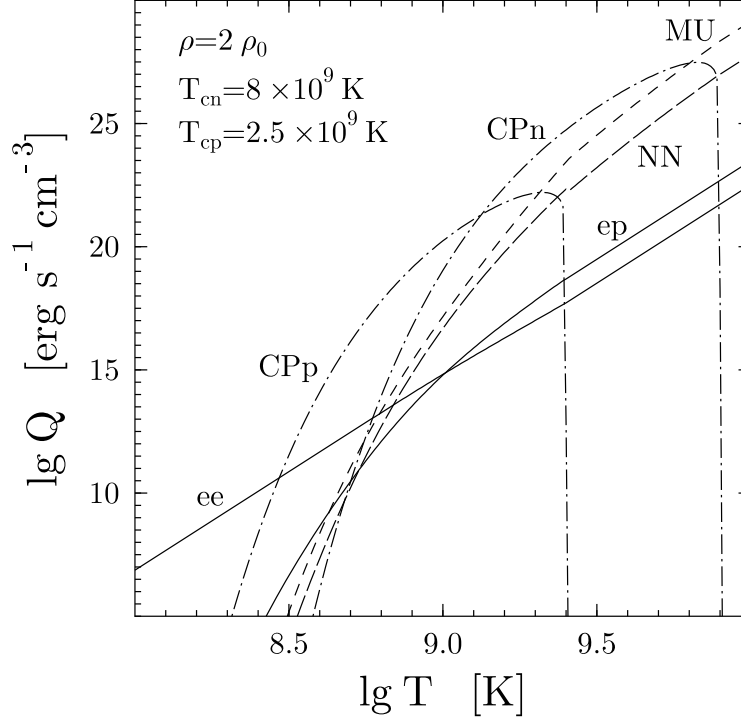


Fig. 1. Temperature dependence of neutrino energy emission rates for various neutrino reactions in  $npe$  matter at  $\rho = 2\rho_0$ ,  $T_{cn} = 8 \times 10^9$  K and  $T_{cp} = 2.5 \times 10^9$  K. The neutrino reactions are: modified Urca (MU, sum of  $n$  and  $p$  branches), nucleon-nucleon bremsstrahlung (NN, sum of  $nn$ ,  $np$  and  $pp$  branches),  $ee$  and  $ep$  bremsstrahlung, Cooper pairing of neutrons (CPn) and protons (CPp).

In Fig. 1 we show neutrino emission from the modified Urca process (1) (sum of the proton and neutron branches), nucleon-nucleon bremsstrahlung (2) (sum of  $nn$ ,  $np$  and  $pp$  reactions), Cooper pairing of neutrons and protons (4), and  $ep$  and  $ee$  bremsstrahlung processes (5) and (6). The emissivities in the last two reactions are obtained in Sects. 4 and 5. The emissivities of the modified Urca and nucleon-nucleon bremsstrahlung reactions (1) and (2) are taken as from Levenfish & Yakovlev [7], with proper account for suppression of the reactions by the neutron and proton superfluidities [3]. The neutrino energy emission rate due to pairing of neutrons is plotted in ac-

cordance with the results by Yakovlev et al. [11, 12]. The neutrino emission due to pairing of protons is calculated taking into account the relativistic corrections [13] to the non-relativistic result [11, 12]. The allowance for the relativistic corrections increases production of neutrinos due to proton pairing by more than one order of magnitude. The neutrino emissivity due to  $ep$  bremsstrahlung is calculated in the *low temperature limit* (see Sect. 4) from Eqs. (40) and (41). We use Eq. (51) to obtain the neutrino emission due to  $ee$  bremsstrahlung.

At  $T > T_{cn}$  the neutron-star matter is nonsuperfluid, so that the modified Urca process and nucleon-nucleon bremsstrahlung play leading roles. It can be seen that the nucleon superfluidity reduces the Urca and bremsstrahlung neutrino reactions involving nucleons ((1), (2), and (5)) at  $T \lesssim 10^9$  K. On the other hand, the nucleon superfluidity produces two bumps of the partial neutrino emissivities at temperatures slightly below two critical temperatures,  $T_{cn}$  and  $T_{cp}$ , due to Cooper pairing of neutrons and protons, respectively. The emission due to pairing of neutrons dominates over other mechanisms at  $T \lesssim 6 \times 10^9$  K, while the emission due to pairing of protons dominates at  $T \lesssim 1.5 \times 10^9$  K. If the Cooper pairing emission were absent, the total neutrino emissivity at  $T \lesssim 10^9$  K would be 2–4 orders of magnitude smaller due to strong suppression by the nucleon superfluidity. The Cooper pairing can easily turn suppression into enhancement at not too low temperatures [11]. However, the Cooper-pairing neutrino reactions are eventually suppressed by superfluidity, when temperature falls down much below the critical temperature of neutrons or protons ( $T \lesssim 0.2 T_{cN}$ ). For  $T \gtrsim 10^9$  K, the neutrino emission due to  $ep$  bremsstrahlung turns out to be more intense than that due to  $ee$  bremsstrahlung but both processes are much weaker than the other neutrino processes. With decreasing  $T$ , the situation becomes drastically different. At  $T \lesssim 2.5 \times 10^8$  K,  $ee$  bremsstrahlung becomes the leading mechanism of neutrino emission since it is the only mechanism which is almost insensitive to the superfluid state of matter and suffers no exponential suppression. Let us emphasize that its role is even more important for stronger superfluidities (for higher  $T_{cn}$  and  $T_{cp}$ ).

In Fig. 2 we plot the contributions from the same neutrino reactions as in Fig. 1 and add the emissivity produced by the powerful direct Urca process (3). The reaction (3) is treated as described by Levenfish & Yakovlev [7], suppressed by nucleon superfluidity as in [21]. The direct Urca process is seen to dominate all other reactions at  $T \gtrsim 2 \times 10^8$  K. However, in spite of its high efficiency in nonsuperfluid matter, it is strongly suppressed at low  $T$  by nucleon superfluidity, so that  $ee$  bremsstrahlung becomes the leading neutrino emission mechanism at  $T \lesssim 2 \times 10^8$  K. Therefore  $ee$  bremsstrahlung can play leading role even in the case of neutrino cooling in which the direct Urca process is open (by momentum conservation rules) but strongly reduced by

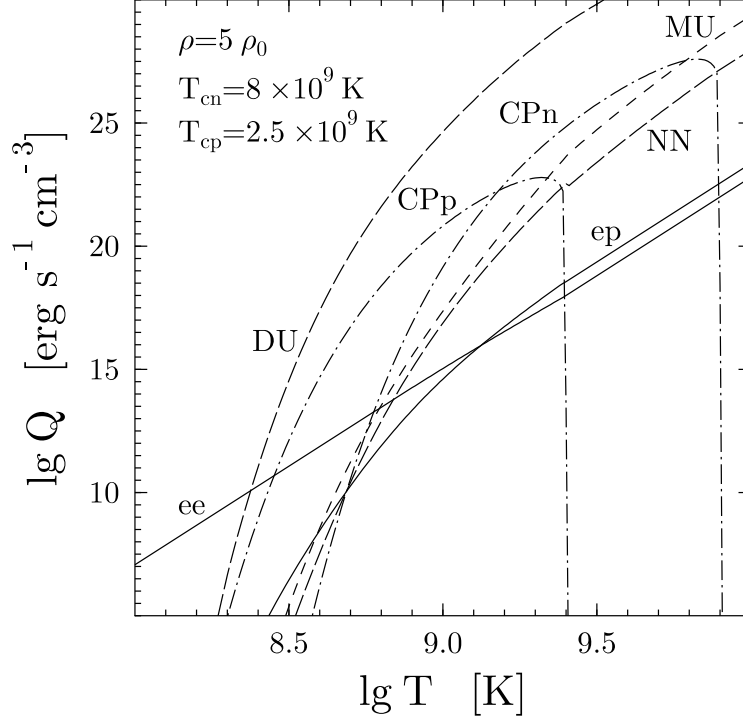


Fig. 2. Same as in Fig. 1 but for  $\rho = 5 \rho_0$ . Direct Urca (DU) process is operative, in addition to neutrino reactions shown in Fig. 1.

superfluidity. Since the superfluidity reduces the direct Urca emissivity, it reduces also strong difference between the standard and enhanced cooling. The temperature range of the  $ee$  bremsstrahlung domination is narrower for rapid cooling.

Figures 3 and 4 display the domains of  $T_{cn}$  and  $T_{cp}$ , where different neutrino production mechanisms dominate at  $T = 2 \times 10^8$  K for the standard and rapid cooling, respectively. Dashes show the lines  $T = T_{cn}$  and  $T = T_{cp}$ . In the left lower squares restricted by these lines, neutron-star matter is non-superfluid. Accordingly, the modified Urca process in Fig. 3 and the direct Urca process in Fig. 4 are the most powerful neutrino reactions in these domains. In the regions to the right of these domains neutrons are superfluid but protons are not, while in the regions above these domains protons are superfluid and neutrons are not. In the upper right squares enclosed by the dashed lines both nucleon species,  $n$  and  $p$ , are superfluid. One can see a variety of dominant mechanisms regulated by superfluidity. If both  $n$  and

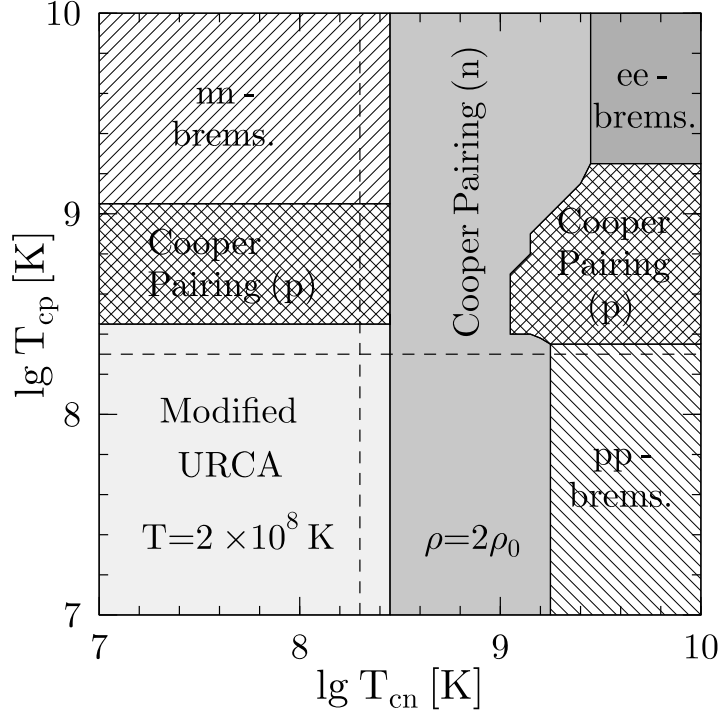


Fig. 3. Domains of the neutron and proton critical temperatures  $T_{cn}$  and  $T_{cp}$  in which different neutrino emission mechanisms dominate in a NS core at  $\rho = 2\rho_0$  and  $T = 2 \times 10^8$  K. Dashes show the lines of  $T = T_{cn}$  and  $T = T_{cp}$ .

$p$  superfluidities are relatively strong (upper right corners of Figs. 3 and 4), they switch off all the neutrino emission mechanisms involving nucleons, and therefore, the neutrino emission due to  $ee$  bremsstrahlung dominates. This region becomes wider with decreasing temperature  $T$  (e.g., during NS cooling). Therefore, one of two reactions considered in this article, neutrino  $ee$  bremsstrahlung, can be the dominant neutrino reaction in both cases of standard and enhanced cooling. We will not discuss all variety of mechanisms which may dominate at different  $T_{cn}, T_{cp}$  and  $T$  but notice that all of them are easily implemented into the cooling codes since their emissivities are described by simple fitting formulae [3, 7, 11, 12, 21]. The present article supplements this description with new neutrino reactions.

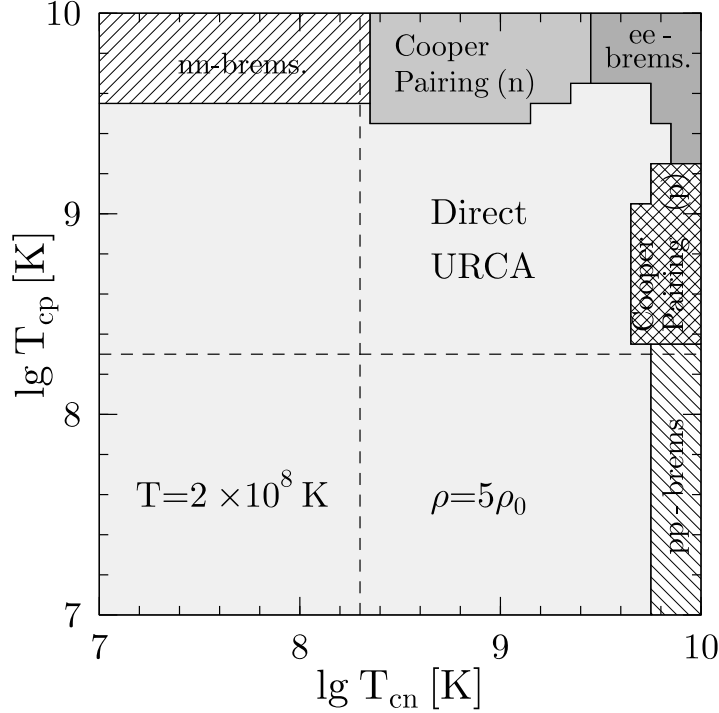


Fig. 4. Same as in Fig. 3 but for the neutrino emission enhanced by the direct Urca process at  $\rho = 5\rho_0$ .

## 7. Conclusions

We have analyzed two neutrino emission mechanisms in the cores of neutron stars: neutrino  $ee$  and  $ep$  bremsstrahlung. We have obtained simple expressions for calculating the neutrino energy emission rates in these reactions (Sects. 4 and 5). We have shown (Sect. 6) that the neutrino  $ee$  bremsstrahlung can dominate in superfluid cores of NSs in some domains of parameters of neutron-star matter. Therefore this reaction should be included in simulations of neutron star cooling.

One may expect that  $ee$  bremsstrahlung will be the main neutrino production mechanism in highly superfluid cores ( $T_{cn} \gtrsim 3 \times 10^9$  K and  $T_{cp} \gtrsim 3 \times 10^9$  K) of sufficiently old NSs (age  $t \gtrsim 10^5$  yr) during the transition from the neutrino cooling stage to the photon cooling stage.

**Acknowledgements.** The authors are very grateful to D.G. Yakovlev for numerous stimulating discussions and for the assistance in the preparation of the text of the present paper. They are also grateful to Kseniya

Levenfish for the assistance in preparation of Figs. 3 and 4. One of the authors (ADK) acknowledges excellent working conditions and hospitality of N. Copernicus Astronomical Center in Warsaw. This work was supported in part by the RBRF (grant No. 99-02-18099a), INTAS (grant No. 96-0542), and KBN (grant 2 P03D 014 13).

## REFERENCES

- [1] Pethick C.J., Rev. Mod. Phys. 64, 1133 (1992).
- [2] Friman B.L., Maxwell O.V., ApJ 232, 541 (1979).
- [3] Yakovlev, D.G., Levenfish, K.P., A&A 297, 717 (1995).
- [4] Lattimer J.M., Prakash M., Pethick C.J., Haensel P., Phys. Rev. Lett. 66, 2701 (1991).
- [5] Takatsuka T., Tamagaki R., Progr. Theor. Phys. Suppl. 112, 27 (1993).
- [6] Takatsuka T., Tamagaki R., Progr. Theor. Phys. 97, 345 (1997).
- [7] Levenfish K.P., Yakovlev D.G., Astron. Lett. 22, 47 (1996).
- [8] Flowers E., Ruderman M., Sutherland P., ApJ 205, 541 (1976).
- [9] Voskresensky D., Senatorov A., Sov. Phys.-JETP 63, 885 (1986).
- [10] Voskresensky D., Senatorov A., Sov. J. Nucl. Phys. 45, 411 (1987).
- [11] Yakovlev D.G., Kaminker A.D., Levenfish K.P., in Neutron Stars and Pulsars, Shibazaki N., Kawai N., Shibata S., Kifune T. (eds.), Universal Academy Press, Tokyo 1998, p. 195.
- [12] Yakovlev D.G., Kaminker A.D., Levenfish K.P., Astron. Astrophys. 343, 650 (1999).
- [13] Kaminker A.D., Haensel P., Yakovlev D.G., submitted to A&A (1999).
- [14] Schaab C., Weber F., Weigel M.K., Glendenning N.K., Nucl. Phys. A605, 531 (1996).
- [15] Kaminker A.D., Yakovlev D.G., Haensel P., A&A 325, 391 (1997).
- [16] Cazzola P., Saggion A., Nuovo Cimento A63, 354 (1969).
- [17] Cazzola P., Saggion A., Nuovo Cimento A63, 367 (1969).
- [18] Lorenz C.P., Ravenhall D.G., Pethick C.J., Phys. Rev. Lett. 70, 379 (1993).
- [19] Lifshitz E.M., Pitaevskii L.P., Statistical Physics, part 2, Pergamon, Oxford 1980.
- [20] Gnedin O.Y., Yakovlev D.G., Nucl. Phys. A582, 697 (1995).
- [21] Levenfish K.P., Yakovlev D.G., Astron. Lett. 20, 43 (1994).
- [22] Berestetskii V.B., Lifshitz E.M., Pitaevskii L.P., Quantum Electrodynamics, Pergamon, Oxford 1982.



- [23] Festa G.G., Ruderman M.A., Phys. Rev. 180, 1227 (1969).
- [24] Haensel P., Kaminker A.D., Yakovlev D.G., A&A 314, 328 (1996).
- [25] Yakovlev D.G., Urpin V.A., Sov. Astron. 24, 303 (1980).
- [26] Haensel P., Urpin V.A., Yakovlev D.G., A&A 229, 133 (1990).
- [27] Prakash M., Ainsworth T.L., Lattimer J.M., Phys. Rev. Lett. 61, 2518 (1988).
- [28] Page D., Applegate J.H., ApJ 394, L17 (1992).
- [29] Tamagaki R., Progr. Theor. Phys. 44, 905 (1970).
- [30] Amundsen L., Østgaard E., Nucl. Phys. A442, 163 (1985).
- [31] Elgarøy Ø., Engvik L., Hiorth-Jensen M., Osnes E., Nucl. Phys. A604, 466 (1996).
- [32] Wambach J., Ainsworth T.L., Pines D., Nucl. Phys. A555, 128 (1993).